Examining diurnal variability across the equatorial Pacific basin associated with ENSO

Tony O. Hurt

Academic Affiliation, Fall 2017: Senior, Jackson State University

SOARS® Summer 2017

Science Research Mentors: Dr. Naoko Sakaeda, Dr. Juliana Dias, Dr. George Kiladis

ABSTRACT

Many questions remain regarding driving mechanisms behind the diurnal cycle across ocean basins and factors that influence it. This study utilizes buoy data to examine diurnal variability of rainfall across the equatorial Pacific basin during the December through February (DJF) seasonal period from 1998 through 2012. Daily mean, diurnal amplitude and phase were calculated for rainfall data assessment and their variability with ENSO phases were examined using composites and probability distributions. Air and sea-surface temperature, relative humidity and surface winds were similarly examined to evaluate potential relationship with the diurnal variability of rainfall. Buoy data were assessed against results from a previous study that performed similar diurnal variability analysis through use of TRMM 3B42 rainfall data. Analysis indicated increased frequency of heavier rainfall during ENSO warm phase (El Niño) events, suggested by larger diurnal amplitude and greater variability in observed rainfall rates across the central Pacific basin. Associated with the increased diurnal amplitude of rainfall rates during El Niño, the diurnal amplitudes of relative humidity and surface winds also increased, while the diurnal amplitudes of air temperature and sea-surface temperature decreased. Observed variability of atmospheric variables was primarily diurnal, although surface pressure and near-surface winds exhibited a semi-diurnal phase signal.

This work was performed under the auspices of the Significant Opportunities in Atmospheric Research and Science Program. SOARS is managed by the University Corporation for Atmospheric Research and is funded by the National Science Foundation, the National Center for Atmospheric Research, the National Oceanic and Atmospheric Administration, the Woods Hole Oceanographic Institute, the Constellation Observing System for Meteorology, Ionosphere, and Climate and the University of Colorado at Boulder.

1. Introduction

Diurnal variability of oceanic and atmospheric variables and its role in the relationship between earth's ocean and atmosphere within the tropics has long been a focus area of research. In large part due to the unprecedented El Niño event of 1982-83, the Tropical Ocean – Global Atmosphere (TOGA) program was launched by the World Climate Research Program in 1985 as an international effort to better understand the relationship between earth's ocean and atmosphere. One of the key objectives of the program was investigating the multi-decadal phenomenon known as El Niño – Southern Oscillation (ENSO), which at the time presented a great challenge due to limited ability to monitor physical processes in equatorial oceanic regions (McPhaden *et al.*, 1998). ENSO, a decadal- to multi-decadal variation in sea-surface temperature (SST) and large-scale wind flow within the equatorial latitudes of the Pacific Ocean basin (Rasmusson and Carpenter, 1982), is generally categorized by three phases – El Niño (anomalous warm SST), La Niña (anomalous cool SST), or neutral (no significant anomalous SST) (Rasmusson and Wallace, 1983).

Initially presented by S.P. Hayes in 1987 as part of the TOGA environmental monitoring program (Hayes *et al.*, 1991), the Tropical Atmosphere Ocean (TAO) buoy array was completed in October 1994 and consisted of 64 Autonomous Temperature Line Acquisition System (ATLAS) moored buoys. Managed by the Pacific Marine Environmental Laboratory (PMEL) and National Data Buoy Center (NDBC), the array spanned the equatorial Pacific basin between the latitudes of 8ºN and 8ºS and the longitudes of 165ºE and 95ºW, with approximate spatial increments of 15º latitude and 2º longitude (McPhaden *et al.*, 1998). The TAO buoy array merged with the Triangle Trans-Ocean buoy network (TRITION) in 2000 and formally become known as the TAO/TRITON network. Maintained and operated by the Japanese Agency for Marine – Earth Science and Technology (JAMSTEC), TRITON consisted of 16 Triangle Trans-Ocean (TTO) buoys between the longitudes of 130ºE and 156ºE, with similar spatial distribution and observation capability as the TAO buoy array (Kuroda, 2002). TAO/TRITON served as the Pacific Ocean branch of the Global Tropical Moored Buoy Array (GTMBA).

Data obtained via TAO buoys has presented researchers with an abundance of detailed information regarding seasonal, monthly, and diurnal variations in oceanic and atmospheric variables. In particular, analysis of these variables indicated an intriguing relationship between ocean and atmosphere. Serra and McPhaden (2004) noted that the diurnal cycle of rainfall influenced the cycle of ocean mixing, which in turn affected air temperature, SST, and upper-ocean heat content. Diurnal variability analysis from the study found that rainfall intensity and frequency typically peaked between 0400 and 0700 local time (LT), with a minimum observed in late afternoon/early evening around 1800 LT. However, the greatest rainfall accumulation occurred during the afternoon at some locations, owing to a maximum in rainfall intensity occurring at that time. Similar to the diurnal variability of rainfall identified by Serra and McPhaden, Ueyama and Deser (2008) determined that the primary near-surface meridional wind variability was diurnal, but zonal wind variability was semi-diurnal, with maximum zonal (westerly) anomalies were observed around 0325 and 1525 LT.

Research into diurnal signal response to ENSO such as Meinen and McPhaden (2000), which concluded that changes in surface winds and SST influenced the volume warm water in the equatorial Pacific basin and ENSO, further illustrated that research of oceanic and atmospheric diurnal signals, particularly their relation to ENSO, was critical to further

understanding the complex relationship between ocean and atmosphere. In attempt to address the relative lack of examination of diurnal variability associated with ENSO, Hurt *et al.* (2016) investigated the diurnal cycle of rainfall over much of the eastern and central Pacific basin through analysis of microwave satellite data obtained from the Tropical Rainfall Measuring Mission (TRMM) and Global Precipitation Measurement (GPM). Findings from the study indicated grater diurnal variability and increased frequency of heavier rainfall across much of the Pacific basin, particularly within the central and eastern regions associated with El Niño, with the opposite occurring in conjunction with La Niña. Repeating the analysis with buoy data offered several differences in comparison with TRMM 3B42 data. Hourly resolution of buoy data versus 3-hourly resolution of TRMM satellite data (Simpson *et al.*, 1988) offered an advantage in temporal resolution, while the 4-meter altitude of buoy measurement instruments offered a closer-range examination of rainfall and additional variables compared to the 400-kilometer measurement altitude of TRMM.

2. Data

This study will use buoy data over the Pacific basin to test the consistency of results found by Hurt et al. (2016), which used TRMM 3B42 data to examine the relationship between the diurnal cycle of rainfall and ENSO. Temporal resolution is one of the primary advantage of offered by buoy data (hourly) compared to TRMM 3B42 data (3-hourly).

Standard ATLAS moorings measured surface wind speed and direction, air temperature, sea-surface temperature (SST) and sub-surface temperature, relative humidity and shortwave radiation at their respective location. Development and testing of NextGeneration ATLAS moorings, which were aimed at improved data quality and reduced costs, commenced in October of 1994, with the first being operationally deployed in 1996. Efforts to upgrade all standard moorings to NextGeneration moorings were completed the following year. In addition to standard mooring measurements, NextGeneration ATLAS moorings also measured barometric pressure, longwave radiation, and rainfall rate. All measurements were 10-minute samples except rainfall, radiation, and barometric pressure, which were one-, two-, and sixty-minute samples, respectively. Data resolution was 0.2 m s^{-1} (surface wind speed), 1.4º (surface wind direction), 0.01ºC (air temperature), 0.001ºC (SST and sub-surface temperature), 0.4% (relative humidity), 0.4 and 0.1 W m^{-2} (short- and longwave radiation), 0.1 hPa (barometric pressure), and 0.2 mm hr^{-1} (rainfall rate). Standard heights for meteorological sensors were 4 meters (wind), 3.5 meters (short- and longwave radiation), and 3 meters (air temperature, relative humidity, barometric pressure) (Guilyardi *et al.,* 2009).

Operational responsibility of the TAO array was transferred from PMEL to NDBC in 2005, and 2011 marked the beginning of the transition to the Refresh system. The Refresh system enabled data transmission of hourly data from moored buoys to NDBC via the Global Telecommunications System (GTS). Data transmission from buoys occurred during two transmit windows daily in order to coincide with satellite passes – from 0600 to 1000 and 1200 to 1600 local solar time (LST) – and also reduce telemetry costs and conserve battery power. Prior to Refresh system availability, buoy data was recorded and stored internally and obtained when buoys were recovered (National Data Buoy Center).

3. Methodology

a. ENSO definition

TAO/TRITON buoy array data were examined to assess the relationship between diurnal variability and ENSO, and the Oceanic Niño Index (ONI) was used to identify ENSO phase. ONI evaluates SST values within the equatorial region between 5° north and 5° south latitude, bounded by the longitudes of 170° and 120° west. Within this region, SST anomalies exceeding ±0.5 degree Celsius serve as the threshold for designation as an El Niño/La Niña event. For increased accuracy in assessment of low-frequency variability of SST, ONI utilizes a three-month (tri-monthly) running mean. Anomalous SST values must exceed the specified threshold for a period of at least five consecutive tri-monthly periods in order for an El Niño or La Niña event to be declared (Trenberth, 1997).

Per ONI definition, five El Niño and four La Niña events were observed during the overall period of study (1998 to 2012). El Niño events occurred during the years of 1998, 2002-03, 2004-2005, 2006-07, and 2009-10. La Niña events occurred during the years of 1998-2001, 2007-08, 2010-11, 2011-12 (Climate Prediction Center). El Niño and La Niña events have historically peaked during the boreal winter months (Soon-Il and Wang, 2001), therefore analysis of diurnal variability within December, January, February (DJF) served as the tri-monthly seasonal assessment period.

b. Diurnal variability analysis and testing

Air temperature, sea surface temperature (SST), rainfall rate, relative humidity, and surface wind variables had the greatest temporal density over the equatorial region of interest. Hourly means for all variables at each buoy location were created by averaging the individual hour during each day throughout the period of study. Daily and seasonal means were also calculated for the study period. Similarly, averages for each variable were created for ENSO phase and climatology throughout the period. ENSO means were then compared to climatological mean values to analyze departure from mean during the period.

Diurnal mean, diurnal amplitude, and diurnal phase for each variable was calculated for each buoy location using the method used in Sakaeda *et al.* (2017). The daily mean represented the daily average of observed hourly data for each location. The diurnal amplitude indicated the difference between the observed maximum value and diurnal mean of a given signal. The diurnal phase represented the time of day that the maximum measured value of a particular variable was observed, in terms of local solar time (LST). To examine climatological values and variability with ENSO, composites of daily mean, diurnal amplitude and phase were calculated for all DJF climatology, El Niño, and La Niña for each buoy location, and also averaged for available buoys within the Niño 3.4 region. This allowed for analysis and comparison of spatial distribution and variability with ENSO through creation of maps displaying the calculated composites. Additionally, TAO/TRITON buoy data were evaluated against results obtained from previous research into the diurnal cycle that was conducted by Hurt *et al.* (2016) using TRMM 3B42 (Huffman *et al.*, 2007) to examine potential differences in observed rainfall.

Probability distributions and composite time series were used to test significance of relationship between DJF climatology, El Niño, and La Niña. Statistical significance of variability in the diurnal amplitude and phase at each buoy location was tested via bootstrap resampling, similar to Sakaeda and Roundy (2014), Roundy *et al.* (2010), Roundy and Frank (2004b), and Wilks (1995). For testing, 1000 bootstrap iterations were performed to ascertain statistically significant difference from zero at the 95% confidence interval.

4. Results

a. The Diurnal Cycle of Rainfall within the Pacific Basin

In this section, we show the mean daily-mean, diurnal amplitude and diurnal phase of rainfall rates at each buoy within the Pacific basin and discuss their variability with ENSO phases and their consistency with the results of Hurt *et al.* (2016) with TRMM 3B42 data.

1.) Daily mean

Figure 1 shows the daily mean of observed rainfall rates at each buoy during all DJF, El Niño, and La Niña. Daily mean of observed rainfall rates exhibited a trend of decreasing values with progression from west to east throughout the equatorial Pacific for all ENSO phases throughout the period of focus. Daily mean values generally fell within the 0.25-0.5 mm hr^1 range during all phases, with a decrease to 0.025-0.25 mm hr^1 within 2° of the equator during La Niña along the longitudinal axis of 165°E. Mean rates ranging from 0.025-0.25 mm hr^1 were observed extending east from the international dateline across the central Pacific basin, although those climatological values represented higher rainfall rates during El Niño and a general lack of rainfall during La Niña. The eastern Pacific east of 140°W exhibited similar rainfall patterns observed with El Niño and La Niña, with the exception of the longitudinal axis of 95°W. Mean rainfall rates there were generally consistent regardless of ENSO phase, with observed daily mean rainfall rates between 0.1-0.5 mm hr^1 north of the equator. Although daily mean rainfall rate values were below 0.025 mm hr^1 south of the equator during El Niño, mean rates during La Niña were between 0.025-0.1 mm hr^1 at corresponding buoy locations.

Differences between the daily mean rain rates are better shown by looking at the anomalies of the daily mean rates from their seasonal cycle at each buoy location (Fig. 2). Daily mean rainfall rate anomalies during El Niño and La Niña were most pronounced in the central region of the Pacific basin, situated along the western edge of the SST anomaly pool and just west of the greatest SST anomalies observed during each ENSO phase. Anomaly magnitude steadily decreased with eastward progression across the basin, ranging from maximum values of 0.25 mm hr^1 along 165°E to within 0.1 mm hr^1 at 140W. These values were consistent with both ENSO phases, with positive rainfall rate anomalies observed during El Niño and negative anomalies observed during La Niña. Anomaly magnitude was greatest along the equator, with decreasing anomalous rainfall rates observed with poleward progression. Along 165°W, observed anomaly values reversed from positive (negative) to negative (positive) during El Niño (La Niña) once poleward progression reached 5°N. A similar trend was observed with poleward progression south of the equator, but the reversal in anomaly did not occur until reaching 10°S. Fewer significant daily mean rainfall rate anomalies were evident in the eastern Pacific, although roughly half of the buoy locations observed anomaly values up to approximately 0.15 mm hr^1.

As was observed in the central Pacific, the poleward fringe of the focus area experienced a reversal of positive (negative) to negative (positive) anomaly values with El Niño (La Niña) for the buoy located at 10°N, 140°W although the anomaly value was generally lower than 0.1 mm hr^{1}. The geographic location of maximum daily mean and mean anomaly values from buoy data match up well with results obtained via TRMM data in Hurt *et al.* (2016).

2.) Diurnal amplitude

Figure 3 represents a similar map as in Fig. 1, except showing the mean diurnal amplitude of rainfall rates. Diurnal amplitude of observed rainfall rates exhibited a west to east trend of increasing amplitude with respect to the mean. West of the international dateline, the diurnal amplitude was approximately the same as the daily mean rainfall rate. However, observed diurnal amplitude in the central and eastern Pacific equatorial region was generally larger than the daily mean, indicative of greater variability in observed rainfall rates. Diurnal amplitude was roughly 0.025-0.05 mm hr^{1} greater than daily mean throughout most of the central Pacific, and approached 0.5 mm hr^{1} at a few buoy locations in the eastern Pacific, particularly along the 95°W longitudinal axis.

Diurnal amplitude anomalies (Fig. 4) exhibited the pattern of daily mean rainfall anomalies across the entire basin, with anomaly values generally about 0.1 mm hr^{1} greater than daily mean values. However, a few eastern Pacific buoys that were located to the east of the greatest SST anomalies within the SST anomaly pool exhibited observations opposite of the general trend across the basin. Diurnal amplitude observed at the buoy located along the equator at 110°W indicated a negative anomaly during El Niño and positive anomaly during La Niña. An additional buoy located at 5°S, 95°W also reflected the same observation. The buoy location of 2°N, 95°W observed a positive diurnal amplitude anomaly during El Niño, but no significant anomaly during La Niña. Compared to findings from Hurt *et al.* (2016), diurnal amplitude and amplitude anomalies indicate very similar measurements between buoy and TRMM data in terms of regions of maximum and minimum amplitude with ENSO as well as anomaly value.

3.) Diurnal phase

Figure 5 shows the diurnal phase that most frequently occurred at each buoy location (mode). The mode is used for this analysis due to the inefficacy of taking an average diurnal phase. Take for example a case where diurnal the diurnal phase tends to occur around midnight; averaging values close to 0000 LST and 2400 LST would yield an average around value around 1200 LST, which is an inaccurate representation what actually occurs. Diurnal phase was most frequently during the overnight and early morning hours over the open ocean. The lone exception was the buoy located along the equator at 125°W, which had a phase around 1200 LST. Although the majority of buoy locations experienced no significant change in phase between El Niño and La Niña, the locations that did exhibit significant change in phase were not limited to any particular region of the basin.

Figure 6 shows the difference between the mode of the diurnal phase during El Niño and La Niña from DJF climatology. Positive anomalies indicate that the rainfall rate tends to peak at a later time than DJF climatology, while negative anomalies indicate that the rainfall rate peaks at an earlier time then DJF climatology. Diurnal phase anomalies (shifts) varied widely across

most of the equatorial Pacific basin, with the western region observing the least varied anomalies. Along the equator at 165°E, observed diurnal phase during El Niño occurred 3 hours earlier (-3 hours) than the mean phase. At the buoy located directly to the south at 2°S, diurnal phase during El Niño was observed 12 hours later (+12 hours) than the mean phase. While neither of the aforementioned buoys experienced phase shifts from mean during La Niña, the buoy at 2°N, 165°E experienced a phase shift of +6 hours during La Niña but no significant phase shift during El Niño. For the remainder of the western Pacific region, phase shifts were generally within +3 hours during El Niño and -6 hours during La Niña. Much of the central Pacific observed phase shifts within 6 hours for both ENSO phases, with a few locations observing phase shifts of 6 to 12 hours. The more significant phase shifts in the central Pacific occurred during La Niña, as buoys along 140°W at 2°N and 2°S observed phase shifts or -12 and -4 hours, respectively. During El Niño, the same buoys observed respective phase shifts of +2 and -8 hours. Variability in diurnal phase continued into the eastern Pacific, where larger phase shifts were observed with El Niño. Phase shifts that were observed during El Niño were greater than 3 hours in most locations, and the sign of the shift varied at all locations in the region. During La Niña in the east Pacific, most observed phase shifts were no greater than -3 hours. A primary exception was the buoy at 2°S, 95°W, which observed a phase shift of +6 hours. There was no evident trend in diurnal phase anomaly with poleward progression, and no straightforward causation leading to the variability across the entire basin. Buoy and TRMM data both reflected the lack of consistent diurnal phase mean or phase anomaly signal throughout the equatorial region, as in Hurt *et al.* (2016).

b. Probability distribution - Niño 3.4 region (Figure 7)

To better understand how the diurnal cycle of rainfall varies with ENSO, this section further examines the variability of the diurnal cycle of rainfall using probability distributions over Niño 3.4 region (Fig. 7). This region was also the region of focus in Hurt *et al.* (2016).

1.) Daily mean

Daily mean rainfall rate distribution suggests a statistically significant relationship between observed daily mean rainfall rates during El Niño and La Niña with climatology, particularly in the central Pacific region (Fig. 7a). Statistical significance is less evident in the eastern Pacific, as climatology and La Niña exhibited very similar distribution (not shown). All rainfall rates above 0.01 mm hr^1 occurred more frequently with El Niño across the entire basin, with the climatological daily mean probability nestled between El Niño and La Niña. This suggests that days with rainfall are more likely during El Niño than with La Niña.

2.) Diurnal amplitude

Diurnal amplitude distribution revealed much less spread in diurnal amplitude probability between climatology, El Niño and La Niña (Fig. 7b). The statistical significance of the relationship of between them is notable at diurnal amplitudes greater than 0.1 mm hr^1 in the central Pacific region. Much like the daily mean distribution in the eastern Pacific, climatology and La Niña exhibited very similar distributions, but diurnal amplitude during El Niño was also very similar to climatology and La Niña in the region. As in Hurt *et al.* (2016), in contrast to the

probability distribution of daily mean that shows increased probability of all daily mean rates during El Niño (Fig. 7a), Fig. 7b shows increased probability of diurnal amplitude above around 0.1 mm hr^1 during El Niño and less than 0.1 mm hr^1 during La Niña.

3.) Diurnal phase

Diurnal phase distribution suggested no statistically significant relationship between climatology, El Niño, and La Niña in the Niño 3.4 region (Fig. 7c) and also over the western Pacific basin (not shown). There was little discernible difference in any of their distributions across that particular region. Diurnal phase generally occurred between 0300 and 0900 LST for DJF climatology and during La Niña, and between 0000 and 0600 LST during El Niño, with the hours between 1200 and 2100 least favored for diurnal phase. There was a very subtle uptick in phase probability between 2100 and 0000 LST during La Niña, which was the only significant difference of phase distribution in the western and central Pacific. Diurnal phase distribution in the eastern Pacific exhibited greater spread in probability, particularly during El Niño. Much like in the western and central Pacific, diurnal phase distribution during El Niño suggested a primary phase between 0300 and 0900 LST, with the afternoon hours between 1200 and 2100 again least favored for diurnal phase. However, phase distribution for climatology and La Niña indicated an equally favored early morning phase between 0300 and 0900 and late evening phase between the hours of 2100 and 0000 LST. Unlike the similarities of diurnal phase between DJF climatology and El Niño in Hurt *et al.* (2016), distribution of diurnal phase from buoy data for DJF climatology and El Niño exhibited greater differences in their diurnal cycles, most notably between 1200 and 2400 LST and again between 0000 and 0300 LST.

c. Relationship with other atmospheric variables

This section examines the diurnal cycle of near-surface winds, temperature, SST, and relative humidity to discuss their potential relationship with the variability of the diurnal cycle of rainfall rate with ENSO.

1.) Meridional and zonal surface winds

Daily mean meridional surface wind climatological values from buoys reflected an axis of convergence across the majority of the basin situated along and just north of the equator (not shown), as also shown by Ueyama and Deser (2008). However, there were notable differences south of the equator, where a band of northerly flow existed from the western Pacific eastward into the central Pacific to near 150°W, indicative of the South Pacific Convergence Zone. The remainder of the central through eastern Pacific was dominated by southerly cross-equatorial flow within the tropics. Negative daily mean anomalies indicated anomalous northerly flow north of the equator throughout much of the western and central pacific during El Niño, with a small swath of anomalous southerly flow located between 5°S-10°S near the dateline. This region of enhanced meridional surface wind convergence coincides with the much of the area of enhanced rainfall that was observed during El Niño. The same region experienced enhanced surface meridional wind divergence during La Niña, which also matched up well with the area of decreased rainfall observed during the associated ENSO phase.

Similar to meridional wind mean, amplitude, and anomalies associated with ENSO, zonal surface wind exhibited greatest anomalous flow within the western and central Pacific as well (not shown). A key observation was that the daily mean zonal flow was primarily easterly across the majority of the equatorial Pacific during La Niña, but during El Niño the easterly flow weakened with westward progression within the central Pacific before becoming westerly along the dateline and locations west of there. This could be a source of further contribution to the increased frequency and intensity of rainfall within the region during El Niño through additional convergence. One of the driving factors behind the zonal surface wind anomalies appears to be background surface pressures observed across the Pacific basin during each ENSO phase, with anomalously high daily mean surface pressures across the western Pacific during El Niño and negative anomalies associated with La Niña.

Anomalies were primarily confined to daily mean values, and only a handful of buoys exhibited significant changes in surface pressure diurnal amplitude associated with ENSO. Composite time series analysis indicated semi-diurnal phase for surface pressure (Fig. 8) and near-surface zonal surface wind (Fig. 9), although near-surface meridional wind tended to indicate more of a diurnal phase (Fig. 10). Interesting to note, however, was the relative spread in the near-surface zonal wind anomaly from daily mean in Figure 9 compared to the uniformity observed with surface pressure in Figure 8. This could indicate additional influence on the near-zonal surface wind outside of surface pressure, although further research would be necessary for greater evaluation.

2.) Relative humidity, air and sea-surface temperatures

Observations of relative humidity, air temperature, and sea-surface temperature between El Niño indicated particular spatial patterns in daily mean and diurnal amplitude (not shown). Daily mean SST indicated warmer anomalies during El Niño and cooler anomalies during La Niña across the central and eastern equatorial Pacific regions. Across the same regions, however, daily mean relative humidity was anomalously lower during El Niño and higher during La Niña. When comparing relative humidity anomalies in diurnal amplitude between the respective ENSO phases, greatest anomaly values were observed at buoys in the central and western Pacific. Increased relative humidity diurnal amplitudes coincided with the enhanced area of rainfall in the central and western Pacific during El Niño, and decreased diurnal amplitudes were associated with La Niña within the same region (Fig. 11). Also notable was that the positive and negative relative humidity anomalies generally coincided with positive and negative air temperature anomalies for diurnal amplitude depicted in Figure 12. Sea surface temperature diurnal amplitude (Fig. 13) tended to be minimized within the region of maximized relative humidity and air temperature amplitude anomalies, and maximized in the region of minimized relative humidity and air temperature anomalies. Greatest sea surface temperature diurnal amplitude anomalies were observed at the western and eastern periphery of the Pacific basin, while greatest amplitude anomalies for relative humidity and air temperature occurred toward the central part of the basin. There were few significant changes in the diurnal phase observed with relative humidity, air temperature, or sea surface temperature.

5. Summary and Conclusion

Despite differences in temporal resolution, rainfall rate data measured by buoys closely matched measurements obtained via TRMM/GPM in terms of location and intensity (see Hurt *et al.* 2016 for comparison). Daily mean and diurnal amplitude anomaly values obtained from both observation platforms indicated similar departures from climatology and the oceanic regions in which they occurred. Central and eastern regions of the basin were the favored areas for wetter than normal conditions during El Niño and drier than normal conditions during La Niña. Although hinted at but not entirely discernible through analysis of buoy data, the SPCZ was clearly visible in satellite rainfall rate data analysis. Also evident in probability distribution analysis is buoy ability to better resolve lighter intensities of rainfall. At common rainfall rate intensities, diurnal amplitude distribution was very similar between observed data from buoys and TRMM. Diurnal phase distribution exhibited much less similarity between platforms, possibly affected somewhat by temporal resolution, as the morning phase near 0600 LST was the most notable similarity between buoy and satellite observations.

Probability distributions of diurnal amplitude indicated that rainfall, relative humidity, near-surface winds, and air temperature experienced more variability within the Niño 3.4 region during El Niño, and exhibited greater daily mean values compared to DJF climatology and La Nina as well. While sea-surface temperature also exhibited greater daily mean values during El Niño, its diurnal amplitude distribution suggested decreased variability during El Niño compared to DJF climatology and La Niña (Fig. 14). Surface pressure had the least variability between DJF climatology and ENSO from amplitude analysis, but greatest variation in diurnal phase distribution between 0000 and 0900 LST, when the most frequent rainfall diurnal phase occurred for DJF climatology and ENSO. For the remainder of the assessed variables, near-surface winds exhibited the greatest variability in diurnal phase, although very little significant difference was indicated.

Overall, buoy-measured rainfall data analyzed in this study are in general agreement with previous studies investigating diurnal variability of rainfall within the tropics through satellite and additional buoy datasets. Coupled with related studies, it can be concluded that there is a large degree of diurnal variability within the equatorial Pacific basin, notably with rainfall. Results from this research demonstrated the highly variable nature of tropical rainfall exhibited through analysis of its daily mean, diurnal amplitude and phase at various locations throughout the tropics. While general assumptions could be drawn from the results connecting the daily mean and diurnal amplitude with diurnal variations in other atmospheric variables such temperature, humidity, pressure and wind, the observed diurnal phase lends itself to a bit more uncertainty in the search for greater understanding of its governing principles. Furthermore, additional research into the driving mechanisms of the diurnal variability of each of these atmospheric variables remains necessary in order to fully understand the scope and magnitude of the physical processes that likely hold a critical role in climate variability.

FIGURES

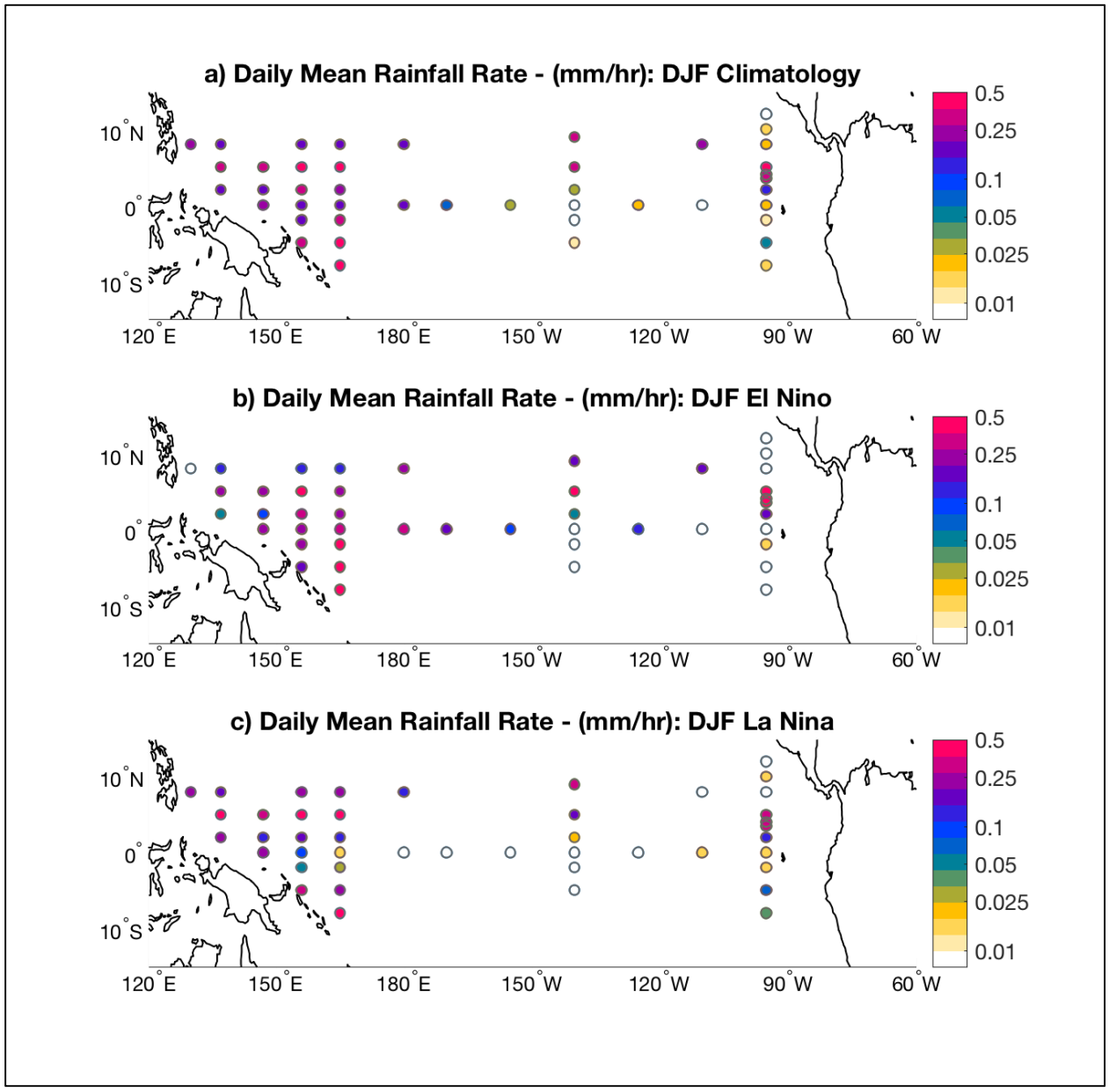

Figure 1. Mean 1998-2012 daily mean rainfall rates (mm hr^{1}) at buoy locations for a) climatology, b) El Niño, c) La Niña.

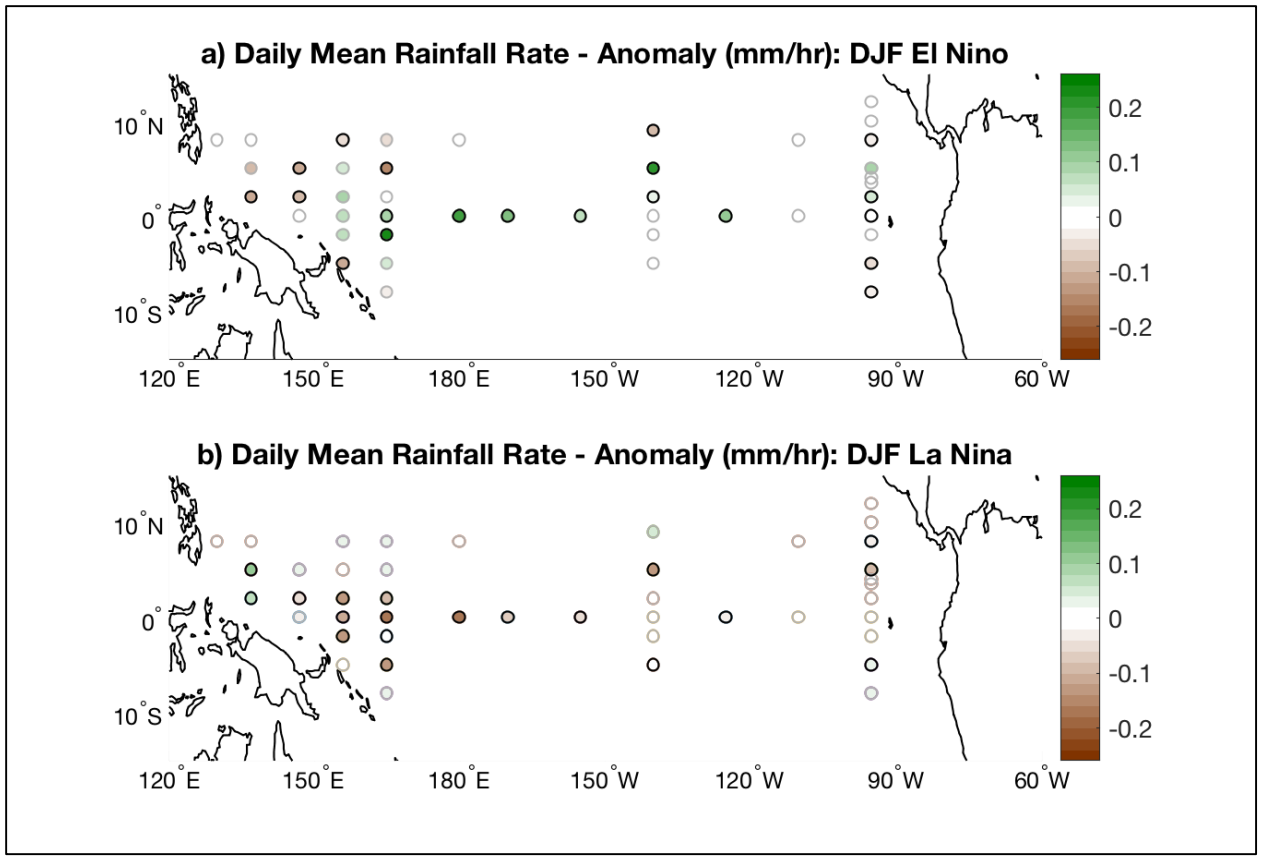

Figure 2. Mean 1998-2012 daily rainfall rate anomaly (mm hr^{1}) at buoy locations during a) El Niño and b) La Niña.

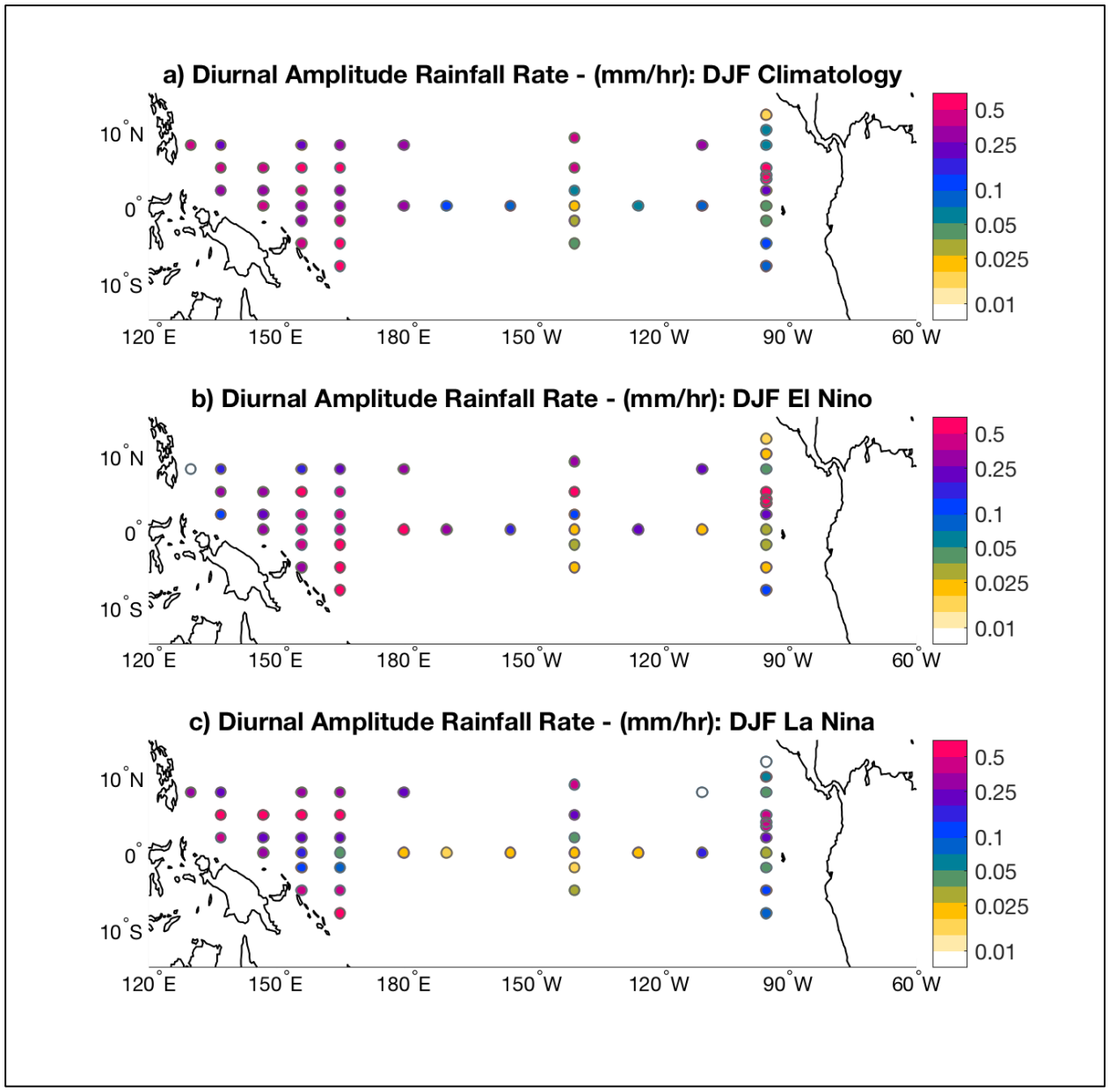

Figure 3. Mean 1998-2012 rainfall rate diurnal amplitude (mm hr^1) at buoy locations for a) climatology, b) El Niño, c) La Niña.

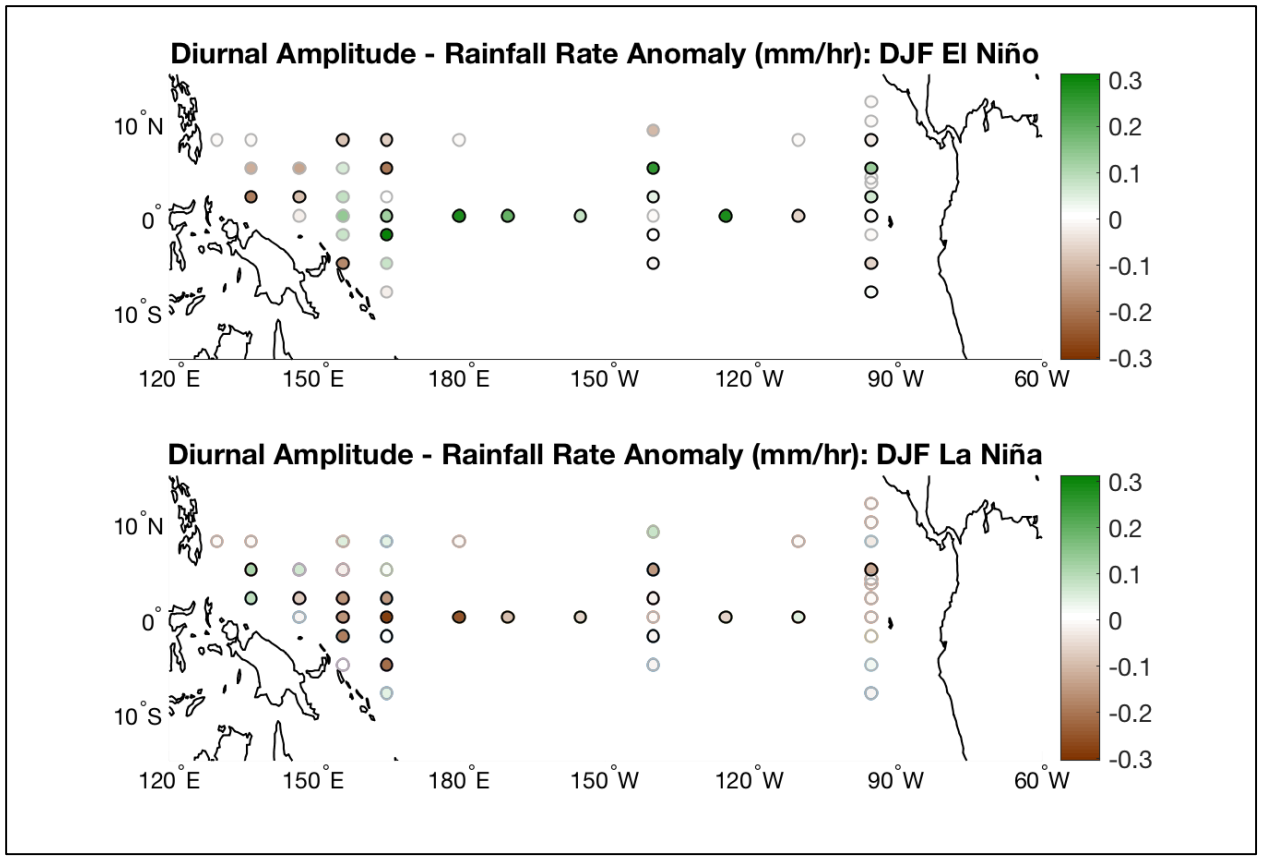

Figure 4. Mean 1998-2012 rainfall rate diurnal amplitude anomaly (mm hr^{1}) at buoy locations during a) El Niño and b) La Niña.

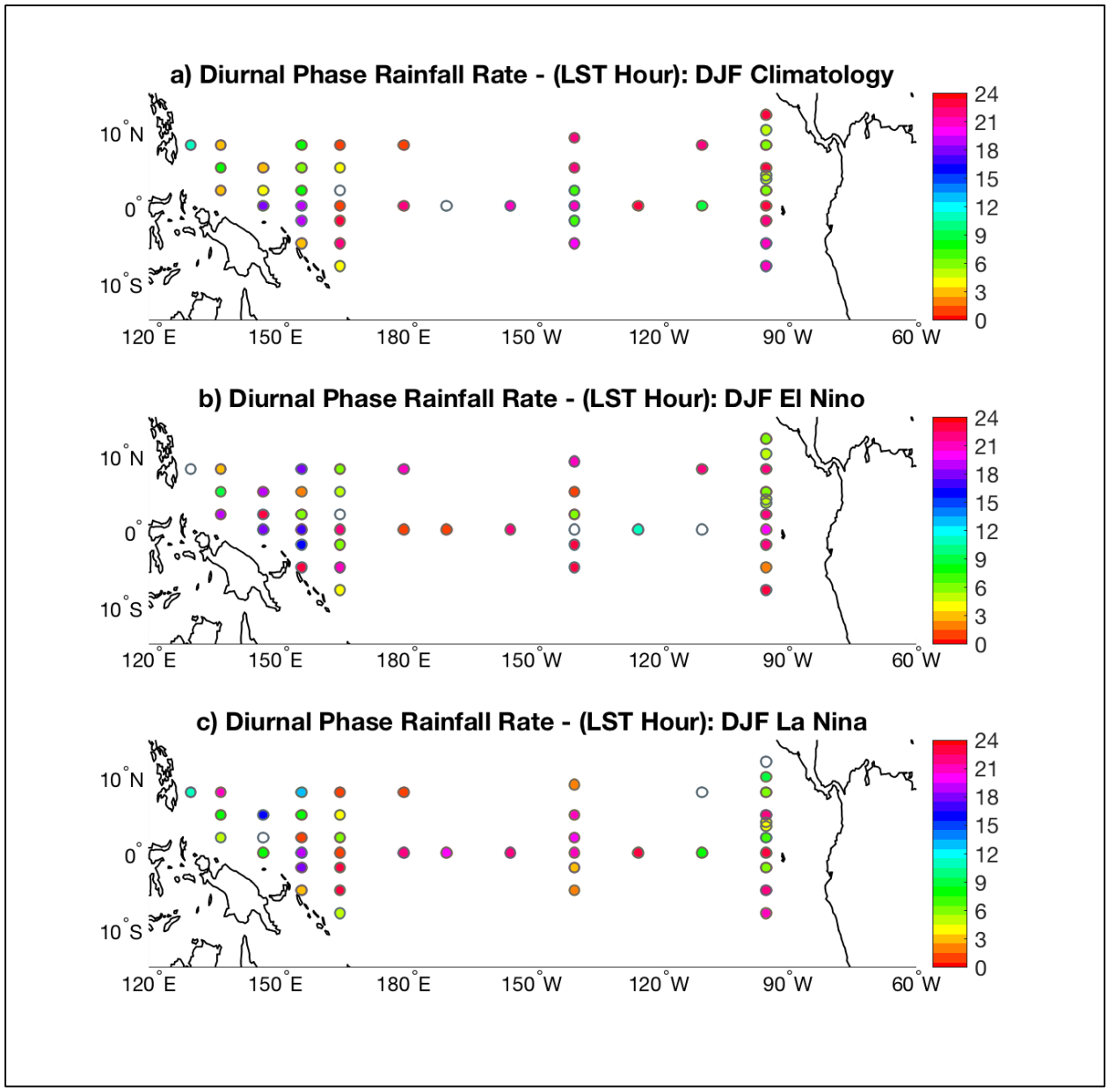

Figure 5. Mean 1998-2012 rainfall rate diurnal phase (LST) at buoy locations for a) climatology, b) El Niño, c) La Niña.

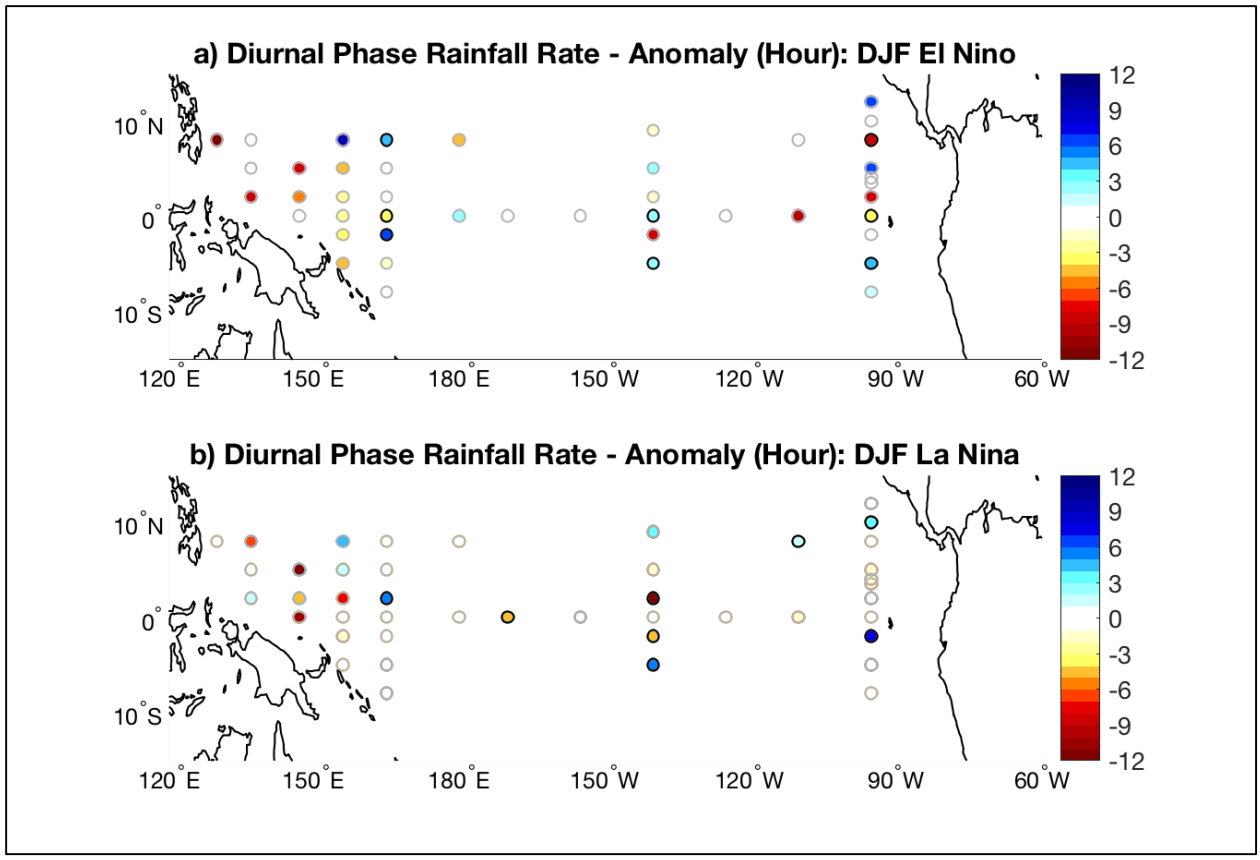

Figure 6. Mean 1998-2012 rainfall rate diurnal phase anomaly (hours) at buoy locations during a) El Niño and b) La Niña.

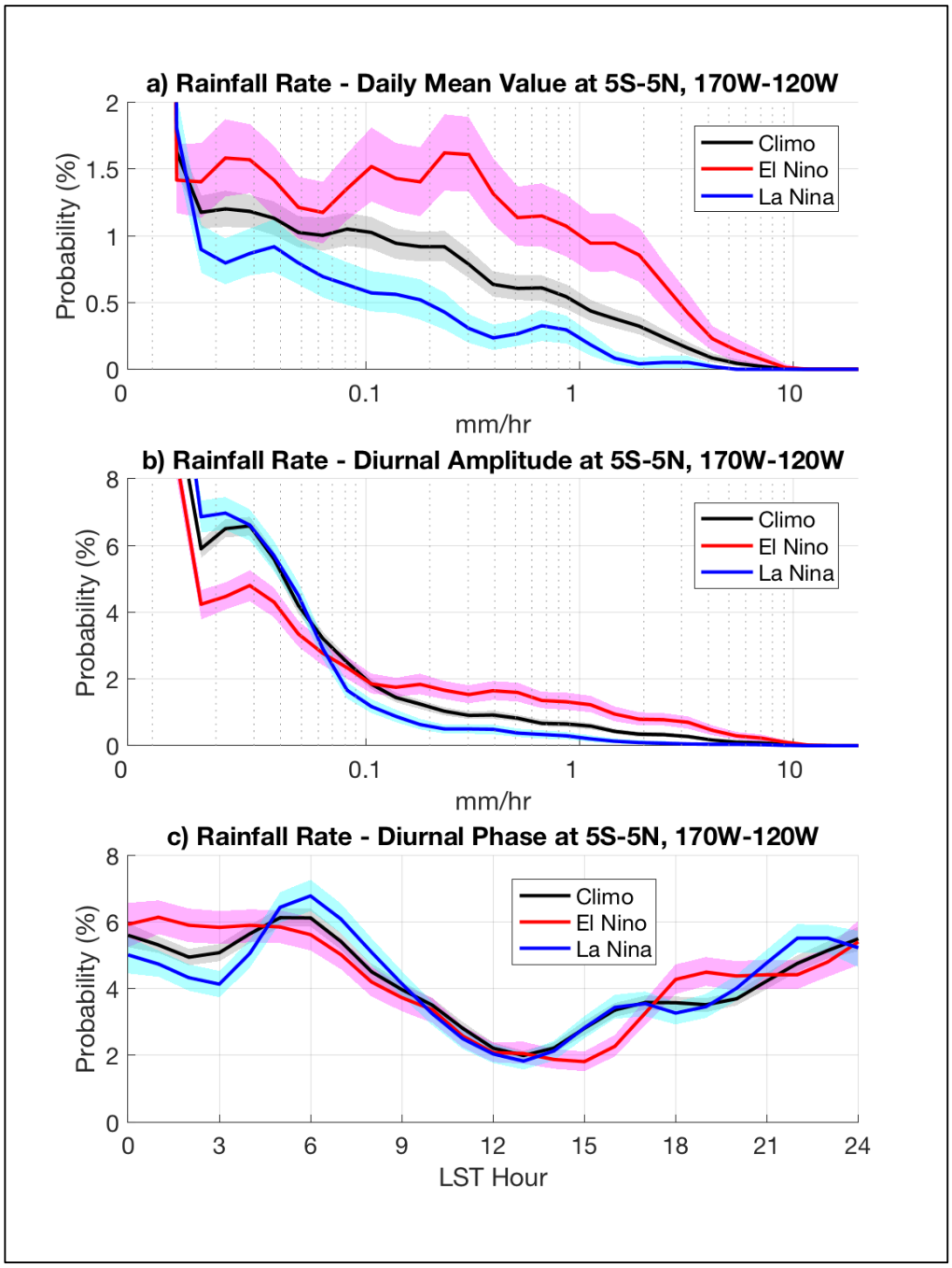

Figure 7. 1998-2012 probability distribution of rainfall rate a) daily mean (mm hr^1), b) diurnal amplitude (mm hr^1), c) diurnal phase (LST hour) within the Niño 3.4 region (8 buoys), with 95% confidence interval shaded.

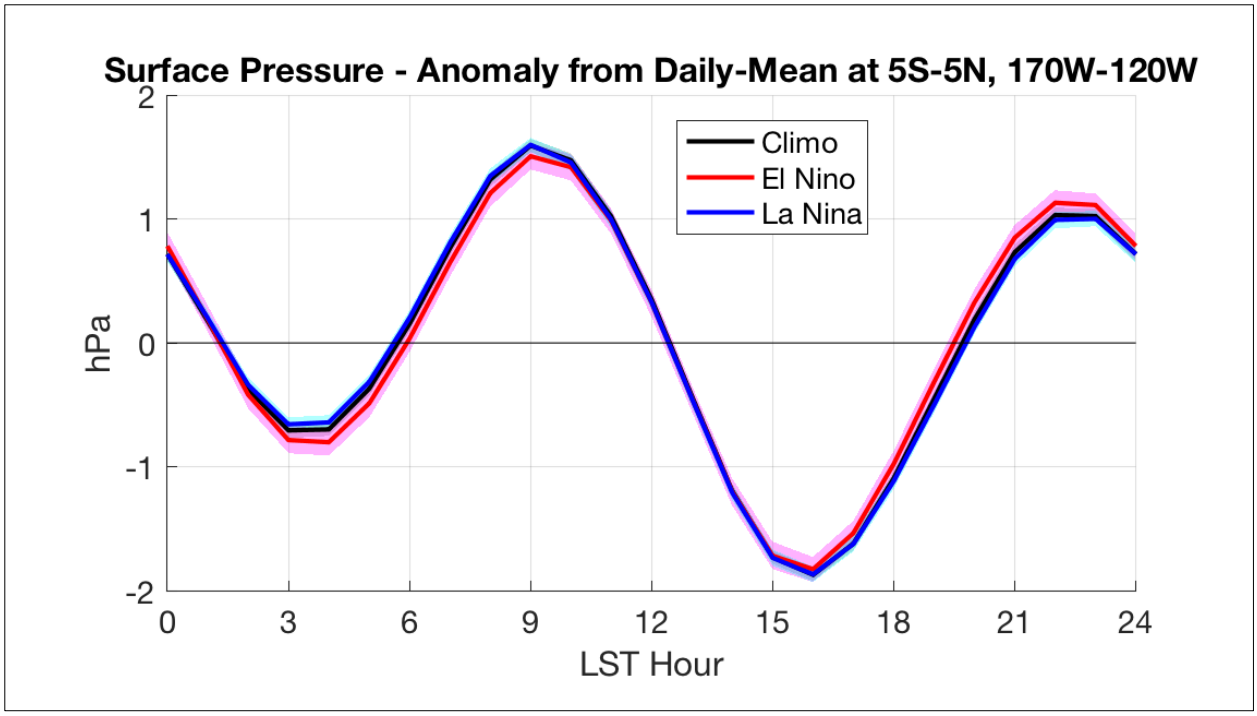

Figure 8. 1998-2012 composite time series of surface pressure anomaly from daily mean (hPa) within the Niño 3.4 region (20 buoys), with 95% confidence interval shaded.

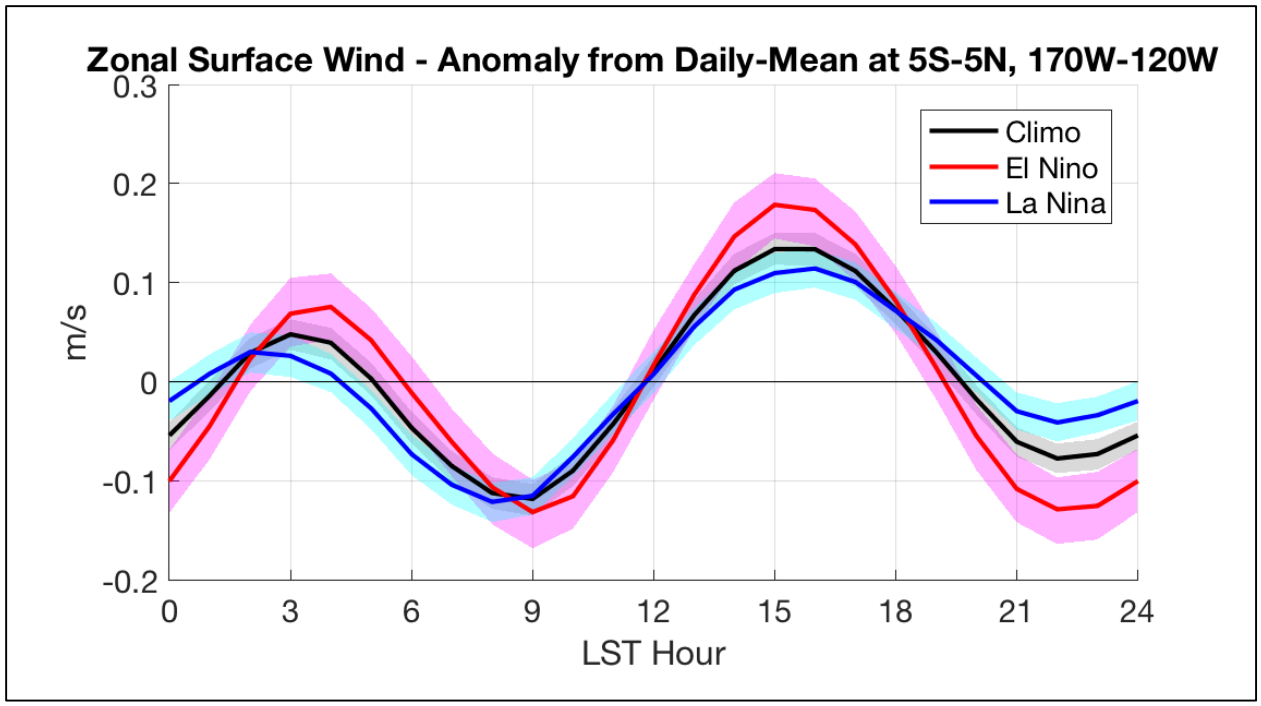

Figure 9. 1998-2012 composite time series of mean near-surface zonal wind anomaly from daily mean (m s^{1}) within the Niño 3.4 region (20 buoys), with 95% confidence interval shaded.

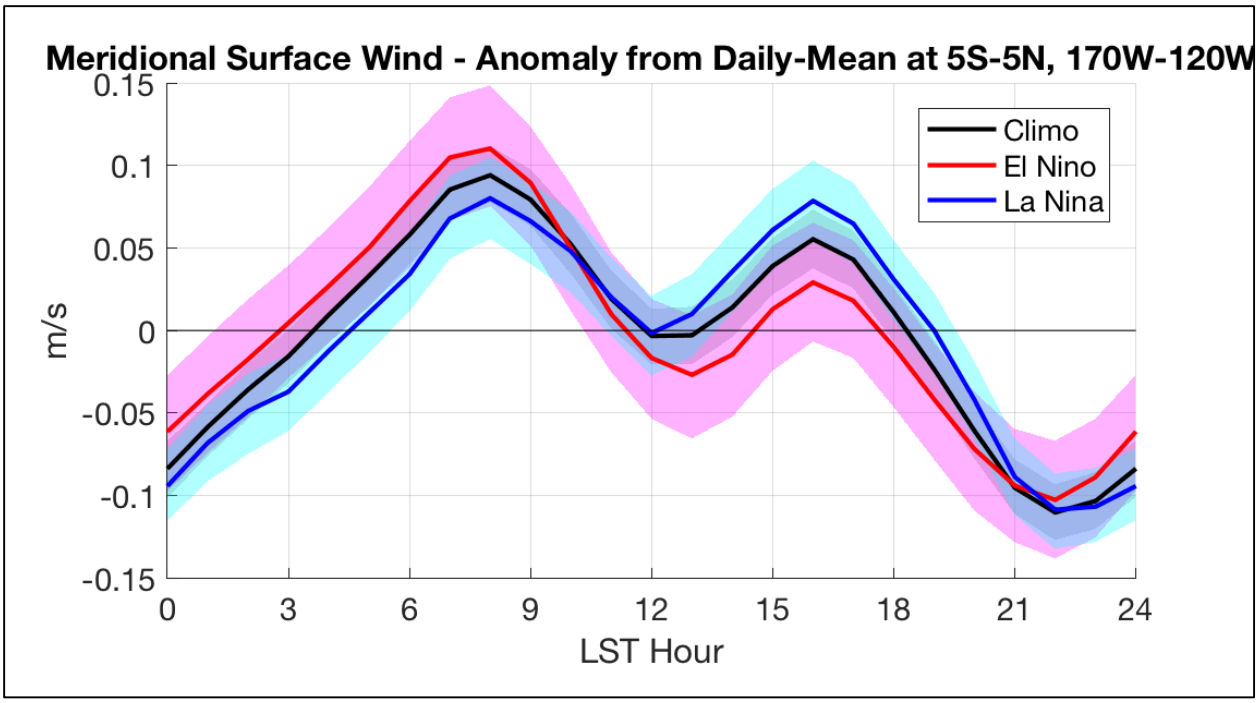

Figure 10. 1998-2012 composite time series of mean near-surface meridional wind anomaly from daily mean (m s^{1}) within the Niño 3.4 region (20 buoys), with 95% confidence interval shaded.

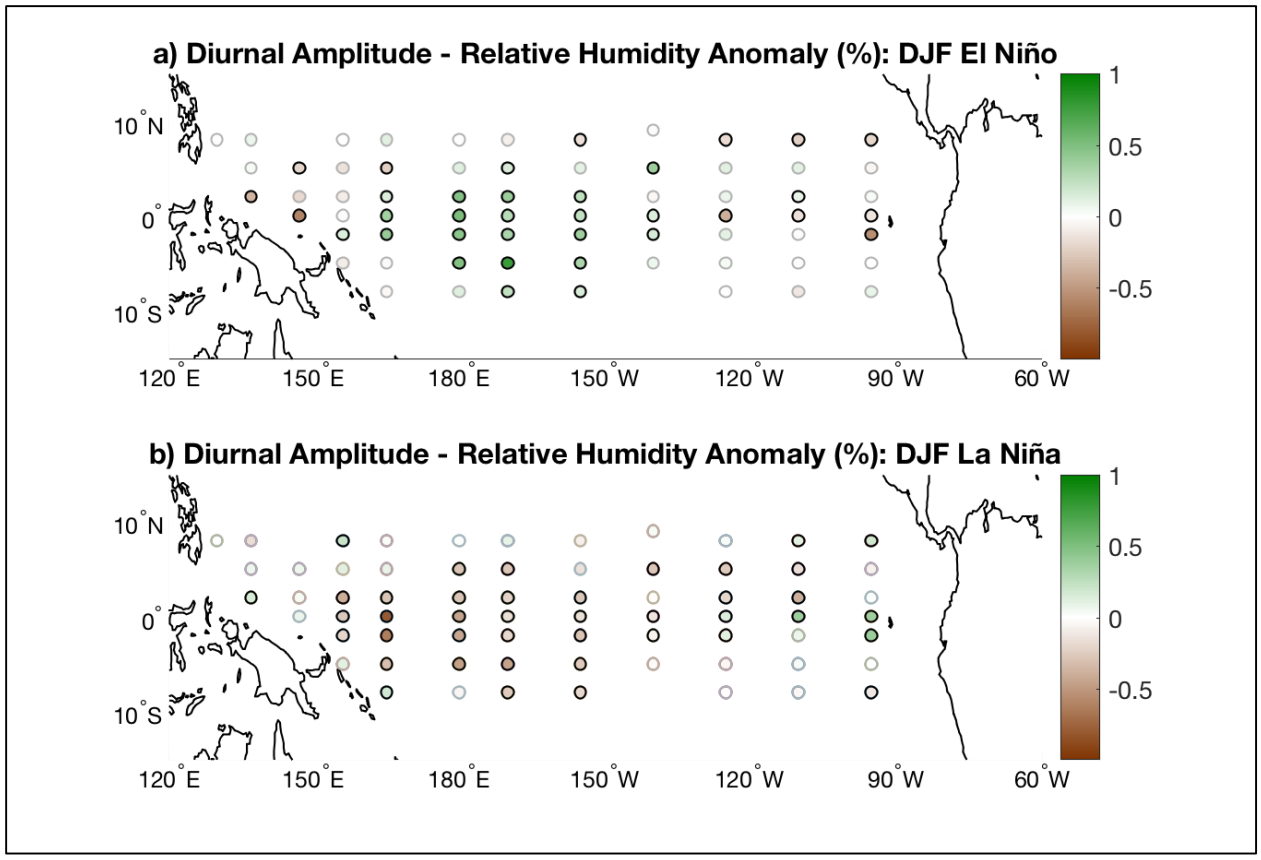

Figure 11. Mean 1998-2012 relative humidity diurnal amplitude anomaly (%) at buoy locations during a) El Niño and b) La Niña.

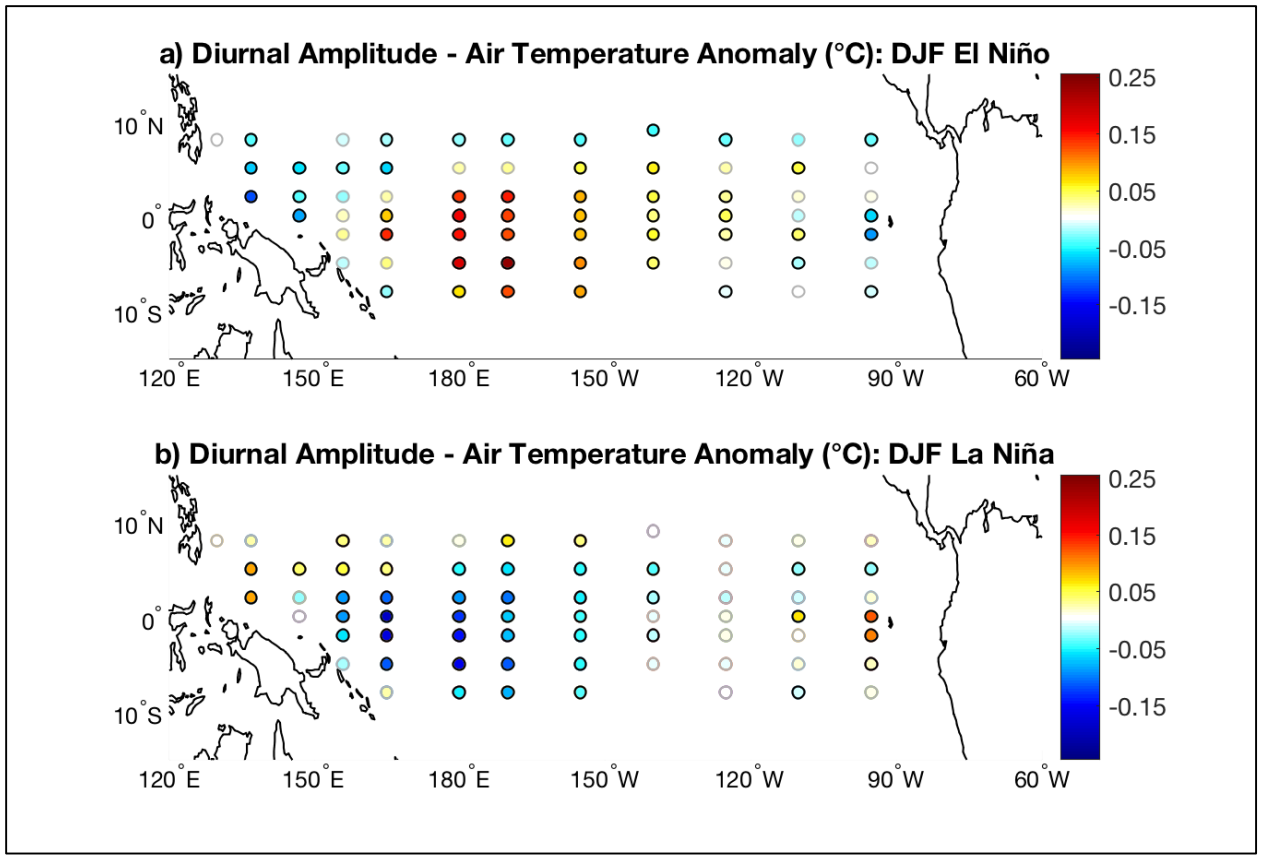

Figure 12. Mean 1998-2012 air temperature diurnal amplitude anomaly (°C) at buoy locations during a) El Niño and b) La Niña.

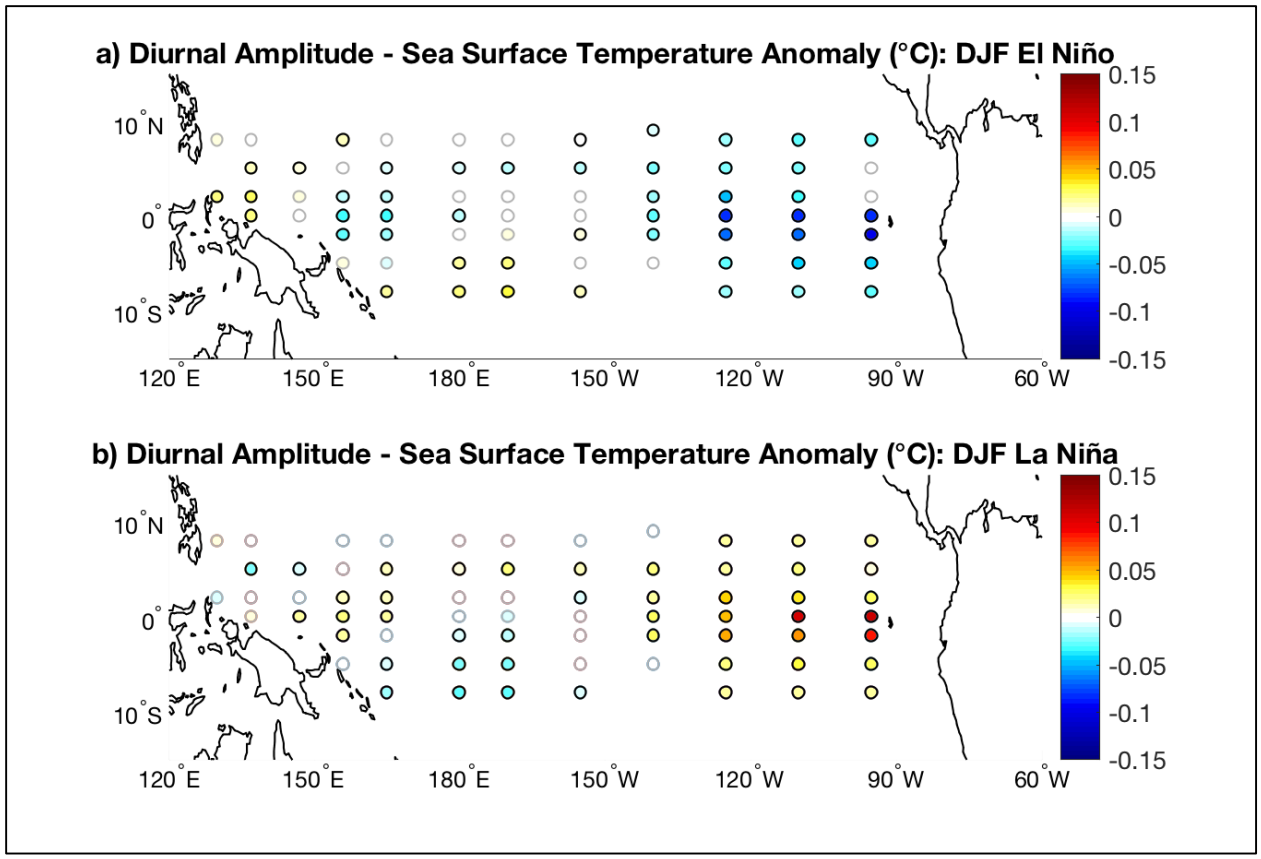

Figure 13. Mean 1998-2012 sea surface temperature diurnal amplitude anomaly (°C) at buoy locations during a) El Niño and b) La Niña.

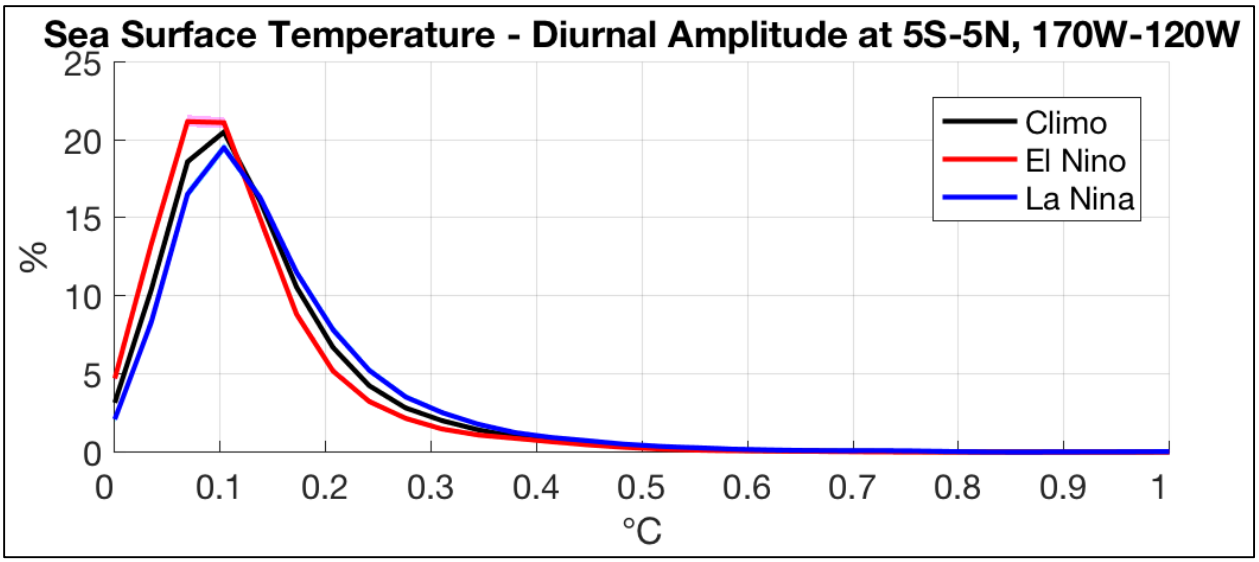

Figure 14. 1998-2012 probability distribution of sea-surface temperature diurnal amplitude (°C) within the Niño 3.4 region.

REFERENCES

Climate Prediction Center *(*2017*),* Oceanic Niño Index (ONI)*, Natl. Weather Serv.,* College Park, Md.

Guilyardi, E., A. Wittenberg, A. Fedorov, M. Collins, C. Wang, A. Capotondi, G. J. van Oldenborgh, and T. Stockdale, 2009: Understanding El Niño in ocean–atmosphere general circulation models: Progress and challenges. *Bull. Amer. Meteor. Soc.*, **90**, 325–340.

Hayes, S. P., L. J. Mangum, J. Picaut, A. Sumi, and K. Takeuchi, 1991: TOGA-TAO: A moored array for real-time measurements in the tropical Pacific Ocean. *Bull. Amer. Meteor. Soc.*, **72**, 339–347.

Huffman, G.J., and Coauthors, 2007: The TRMM multi-satellite precipitation analysis (TMPA): Quasi-global, multiyear, combined-sensor precipitation estimates at fine scales. *J. Hydrometeor.,* **8.1,** 38-55.

Hurt, T.O., J. Dias, G. N. Kiladis, and N. Sakaeda, 2016: Examining the variability of the diurnal cycle of rainfall over the Pacific basin associated with El Niño. *NCAR's Open Sky*, (insert pages here).

Kuroda, Y., 2002: TRITON: Present status and future plan. Report for the International Workshop for Review of the Tropical Moored Buoy Network, JAMSTEC, 77 pp.

McPhaden, M. J., and Coauthors. 1998: The tropical ocean global atmosphere (TOGA) observing system: A decade of progress. *J. Geophys. Res.*, **103,** 14169–14240.

Meinen, C. S., and M. J. McPhaden, 2000: Observations of warm water volume changes in the equatorial Pacific and their relationship to El Niño and La Niña. *J. Climate*, **13**, 3551–3559.

National Data Buoy Center *(*2017*),* Tropical Atmosphere Ocean (TAO) Array, *Natl. Weather Serv.,* Stennis Space Center, Ms.

Rasmusson, E.M., and J.M. Wallace, 1983: Meteorological aspects of the El Nino/southern oscillation. *Science,* **222.4629,** 1195-1202.

Rasmusson, E.M., and T.H. Carpenter, 1982: Variations in tropical sea surface temperature and surface wind fields associated with the Southern Oscillation/El Niño. *Mon. Wea. Rev.,* **110.5**, 354-384.

Roundy, P. E., and W. M. Frank, 2004b: Effects of low-frequency wave interactions on intraseasonal oscillations. *J. Atmos. Sci.*, **61**, 3025–3040.

Roundy, P. E., K. MacRitchie, J. Asuma, and T. Melino, 2010: Modulation of the global atmospheric circulation by combined activity in the Madden–Julian oscillation and the El Niño–Southern Oscillation during boreal winter. *J. Climate*, **23**, 4045–4059.

Sakaeda, N., and P. E. Roundy, 2014: The role of interactions between multiscale circulations on the observed zonally averaged zonal wind variability associated with the Madden–Julian oscillation. *J. Atmos. Sci.*, **71**, 3816–3836.

Sakaeda, N., G. N. Kiladis, and J. Dias, 2017: The Diurnal Cycle of Tropical Cloudiness and Rainfall Associated with the Madden-Julian Oscillation, *J. Climate*, **30**, 3999-4020.

Serra, Y. L., and M. J. McPhaden, 2004: In situ observations of diurnal variability in rainfall over the tropical Pacific and Atlantic Oceans. *J. Climate*, **17,** 3496–3509.

Simpson, J., R.F. Adler and G.R. North, 1988: A proposed tropical rainfall measuring mission (TRMM) satellite. *Bull. Amer. Meteor. Soc.,* **69**, 278-295.

Soon-Il, A., and B. Wang, 2001: Mechanisms of locking of the El Niño and La Niña mature phases to boreal winter. *J. Climate* **14.9,** 2164-2176.

Trenberth, K. E., 1997: The definition of El Niño. *Bull. Amer. Meteor. Soc.*, **78**, 2771–2777.

Ueyama, R., and C. Deser, 2008: A climatology of diurnal and semidiurnal surface wind variations over the tropical Pacific Ocean based on the tropical atmosphere ocean moored buoy array. *J. Climate*, **21**, 593–607.

Wilks, D. S., 1995: *Statistical Methods in the Atmospheric Sciences: An Introduction*. Academic Press, 467 pp.